Capacitance Monitoring of the Infiltration of Ceramic Particulate Preforms with Liquid Metals at 750 to 850 °C

T.R. Jonas, J.A. Cornie, and K.C. Russell

The authors previously developed a capacitance technique to determine the position of the infiltration front as a function of time during the pressure infiltration of ceramic particulate preforms with liquid metals. In the present work, the technique was extended to higher temperatures and was used to monitor the infiltration of alumina particulate preforms with Al-Mg alloys and silicon carbide particulate preforms with Sn and an Al-Si alloy. The infiltration front position could be determined in the alumina preforms. However, it was not possible to clearly interpret the results obtained from the infiltration of semiconducting silicon carbide preforms. The observed range of capacitance circuit voltage to infiltration distance ratios agreed with the predicted range for both simulated and alumina preform infiltration experiments. Formation of unstable infiltration fronts could also be detected.

Keywords
alumina, aluminum alloys, ceramic particulate preforms, metal matrix, silicon carbide

1. Introduction

LIQUID-STATE processes for producing metal-matrix composites combine metal and reinforcement when the metal is molten. Such processes have been proposed as more economical alternatives to solid-state processes such as diffusion bonding and powder metallurgy. Pressure infiltration processes, which use applied pressure to force the liquid metal into a preform of reinforcement material, have already found limited commercial use.

For unidirectional infiltration processes, the ability to monitor the position of the infiltration front allows both process control and study of the fluid flow occurring during the infiltration process. Fluid flow is influenced by the magnitude of the capillary pressure, which is a function of the wetting of the reinforcement by the metal. Therefore, study of the fluid flow also reveals information about the wetting in the system.

Two different techniques have been developed to continuously monitor the infiltration front position during unidirectional pressure infiltration. The first involves inserting a SiC fiber into a nonconducting fiber preform and measuring its resistance during the infiltration experiment.[1-3] As the metal advances into the preform, the length of the fiber contributing to the measured resistance decreases. The second technique, which the authors developed, is noninvasive. An electrode is placed on the outside of the sample tube, and the capacitance between this electrode and the liquid metal on the inside of the tube is measured during infiltration.[4] This second technique was previously tested for temperatures on the order of 300 °C, below the melting point of most alloys of commercial interest.

This article discusses the results obtained using the capacitance technique to monitor the infiltration of alumina particulate preforms with Al-Mg alloys and the infiltration of SiC particulate preforms with Sn and an Al-Si alloy. Most experiments were conducted at 750 °C. The results of infiltration simulation experiments are also examined because they aid in interpreting infiltration results.

T.R. Jonas, J.A. Cornie, and K.C. Russell, Department of Materials Science and Engineering and Materials Processing Center, Massachusetts Institute of Technology, Cambridge, Massachusetts.

2. Basis of the Capacitance Technique

The capacitance technique determines infiltration distance by measuring capacitance during the infiltration process. As illustrated in Fig. 1, a metal signal electrode placed on the outside of the sample tube and the liquid metal inside the tube comprise the capacitor electrodes. The dielectric consists of the sample tube and any gaps between the electrodes and the sample tube. A specially built circuit applies a potential difference between the two electrodes, charging the capacitor. As infiltra-

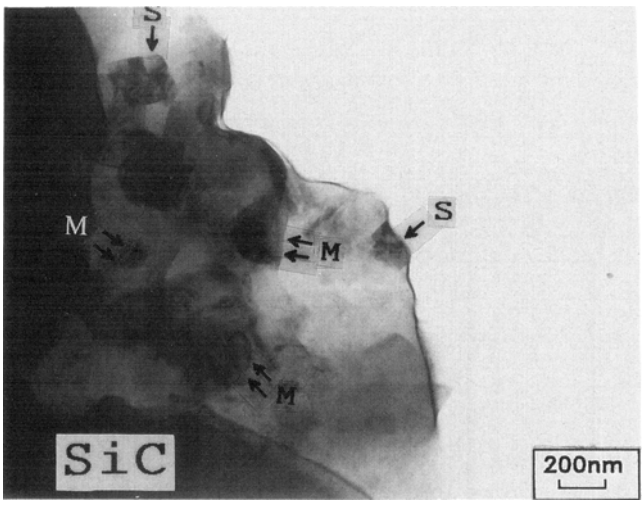

Fig. 1 Schematic of the capacitance technique. The capacitance between the electrodes depends on the effective capacitor length, X, which depends on the infiltration distance.

tion proceeds, the effective capacitor length and thus the capacitance increases. Further details of the technique are given elsewhere.[4,5] Another section of the circuit provides a peak voltage proportional to the capacitance.

For this electrode configuration, the capacitance is proportional to the capacitor length. If end effects can be neglected, the capacitance of a capacitor with coaxial circular cylindrical electrodes and a homogeneous dielectric is given by:

$$C = \frac{2\pi K \varepsilon_o L}{\ln\left(\frac{r_1}{r_0}\right)} \quad [1]$$

In Eq 1, K is the dielectric constant; ε_o is the permeability of free space; L is the capacitor length; r_1 is the radius of the outer conductor; and r_0 is the radius of the inner conductor. In the infiltration experiments, the dielectric was not homogeneous, but consisted of both the sample tube and a gap between the signal electrode and the sample tube. For a coaxial geometry, the capacitance becomes:

$$C = \frac{2\pi \varepsilon_o L}{\frac{1}{K_1}\ln\frac{r_1}{r_0} + \frac{1}{K_2}\ln\frac{r_2}{r_1}} \quad [2]$$

where r_0 is the radial position of the inner conductor; r_1 is the radial position of the interface between the inner and outer dielectric; and r_2 is the radial position of the outer conductor. K_1 and K_2 are the dielectric constants of the inner and outer dielectric, respectively. During the infiltration simulation experiments, an additional gap existed between the inner electrode and the sample tube; the appropriate form of Eq 2 therefore contains an additional dielectric term in the denominator.

The presence of gaps allows the electrodes to shift so that the geometry is no longer coaxial, changing the capacitance per unit length, C/L. The expected range of C/L values can be calculated from the solution for the capacitance of hollow cylinders placed one inside the other:[6]

$$\frac{1}{C} = \frac{1}{2\pi K \varepsilon_o L} \cosh^{-1}\left(\frac{a^2 + b^2 - c^2}{2ab}\right) \quad [3]$$

where a is the radius of the inner cylinder; b is the radius of the outer cylinder; and c is the distance between the centers of the cylinders. For constant radii a and b, the capacitance predicted by Eq 3 is minimum when the cylinders are coaxial and maximum when they are nearly in contact. Therefore, the lowest expected capacitance per unit length is for coaxial electrodes. It can also be shown that the capacitance per unit length between any two nonconcentric cylinders placed one inside the other is less than if the outer cylinder were replaced by a concentric cylinder of smaller radius such that the distance between the new outer cylinder and the inner cylinder is equal to the minimum distance between the old outer cylinder and the inner cylinder. Therefore, C/L for a hypothetical signal electrode whose inner diameter is equal to the outer diameter of the sample tube provides one upper bound on the expected capacitance per unit length.

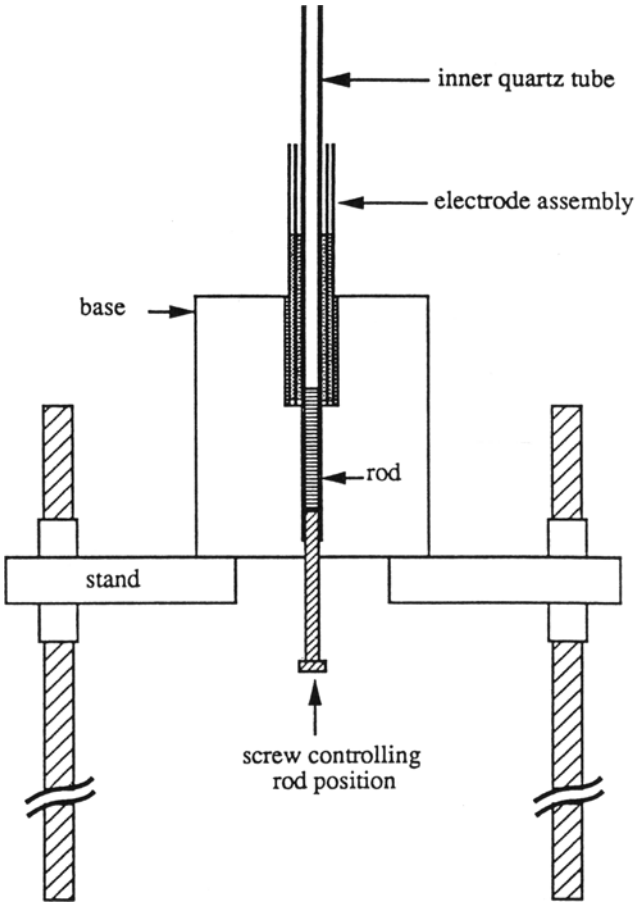

Fig. 2 Schematic of the infiltration simulator. The movement of liquid metal into the preform is simulated by moving an aluminum rod into an empty sample tube.

3. Experimental Materials and Methods

3.1 *Simulation Experiments*

A device that simulated pressure infiltration was used to test the proportionality between the circuit output and the effective capacitor length. The device is shown schematically in Fig. 2. Changes in infiltration distance during the infiltration experiment were simulated by moving an aluminum rod into a quartz tube surrounded by signal and shield electrodes. The 4 cm long aluminum rod, of average diameter 4.85 mm, fit within the 5 mm ID, 8 mm OD by 13.5 cm long inner quartz tube. A screw controlled the position of the rod in the tube and electrically connected it to the base of the device, to which the voltage was applied. The signal electrode consisted of layers of <0.1 mm thick copper sheet wrapped tightly around the inner tube and held in place with a piece of 9 mm ID by 11 mm OD quartz tubing. The signal electrode was approximately 6 cm long and started approximately 2 mm from the bottom end of the quartz

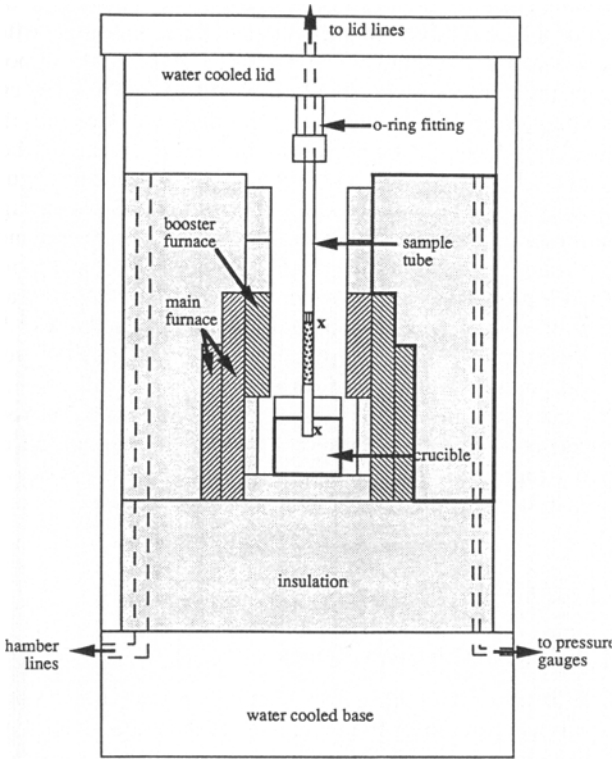

Fig. 3 Schematic of the pressure infiltration unit. The preform is indicated by the small squares inside the sample tube. The electrode assembly for the capacitance technique is not shown. Thermocouple positions are indicated by an x.

tube. The grounded shield electrode was constructed in the same way and held in place with a piece of 12 mm ID by 14 mm OD quartz tubing. Additional copper sheet was wrapped around the outer tube to hold the tube assembly in place in the base of the device. The circuit output peak voltage was measured for several positions of the aluminum rod within the inner tube. The depth of the aluminum rod within the tube was measured with a pair of calipers. Section 4 discusses the simulation results.

3.2 *Infiltration Experiments*

Experiments were conducted with alumina and silicon carbide particles. Sedigraph testing showed both batches of powder to have a median diameter of approximately 9 μm. The powders were packed into preforms with a volume fraction of approximately 0.5. Binderless Saffil alumina paper was placed at the preform entrance after packing to keep the powder in place.

The sample configuration for the two types of preforms was slightly different. The alumina preforms were packed within alumina sample tubes of average ID of 4.88 mm and average OD of 6.27 mm. The silicon carbide preforms were packed within the same quartz sample tubes used in the simulation experiments. For both types of preforms, the nickel signal electrode was formed to fit closely around the sample tube and contained within a slightly larger diameter quartz tube glued to the sample tube. The electrodes used in the alumina experiments had average inner diameters ranging from 6.69 to 6.88 mm. As described previously,[4] alumina insulation was placed on top of the preform to insulate it from the chill rod in thermal contact with the lid of the pressure vessel. For the alumina preform experiments, approximately 0.7 g of titanium granules was placed between the alumina insulation and the chill rod to remove oxygen from the atmosphere.

The pressure infiltration unit used to perform the experiments, illustrated in Fig. 3, was similar to that used in the previous experiments at 300 °C.[4] However, a booster furnace was added to reduce the temperature gradient along the sample. In addition, vacuum gages were installed at the base and lid of the machine for the alumina preform experiments.

The infiltration portion of the experiment consisted of a pressurization step followed by a venting step. First, both the sample tube and the pressure chamber were pressurized with gas. The furnace controls were adjusted until both the upper and lower thermocouples indicated fairly stable temperatures that were within the desired range. Infiltration of the preform was started by venting the gas in the sample tube to atmosphere or to an atmospheric pressure reservoir. Re-equalization of pressure between the sample tube and the pressure chamber halted the infiltration. The creation of a pressure difference between the pressure chamber and the sample tube by venting gas from the sample was necessary to reduce variations in sample temperature during the experiment.

The experimental conditions were different for the two types of preforms. The alumina preforms were infiltrated with Al, Al-2.3 wt% Mg, and Al-5.8 wt% Mg at 750 °C under an argon or nitrogen atmosphere. The Al-2.3 wt% Mg alloy was also tested at 850 °C. Both the pressure chamber and the sample tube were evacuated and backfilled with argon or nitrogen before beginning the infiltration experiment, and the sample tube was vented to an atmospheric pressure reservoir filled with argon or nitrogen. The silicon carbide preforms were infiltrated with Al-12 wt% Si and Sn at 750 °C in air. No special evacuation or venting steps were used.

4. Simulation Experiments

The capacitance circuit voltage was found to be proportional to the amount of positive overlap between the electrodes and thus the effective capacitor length. Figure 4 illustrates the relationship between circuit voltage and electrode overlap obtained for a typical simulation experiment; the conversion factor between circuit voltage and electrode overlap in this experiment was 0.41 V/cm. The conversion factors measured in other experiments ranged from 0.35 to 0.60 V/cm.

The predicted conversion factor between circuit voltage and metal position, V/L, can be obtained by multiplying the expected capacitance per unit length, C/L, by the conversion factor between circuit voltage and capacitance, V/C. The expected capacitance per unit length can be calculated as discussed in Section 2. The dielectric constant of quartz at room temperature is approximately 3.75,[7] and the permittivity of free space is 8.85×10^{-12} F/m. The conversion factor between circuit voltage and capacitance was measured as 0.13 V/pF, so that the theoretically predicted lower bound was 0.33 V/m, whereas the

theoretically predicted upper bound was 0.59 V/cm. The theoretically predicted values compared well with the experimentally observed range of 0.35 to 0.60 V/cm. Therefore, the variation in *V/L* observed experimentally can be explained by the shifting of electrode positions from one experiment to another. The shifting was allowed by the gap between the sample tube and the electrodes.

5. Infiltration Experiments

5.1 *Expected Stages of the Infiltration Process*

Figure 5 schematically shows the physical stages in the infiltration experiment. After both the inside of the tube and the pressure chamber are pressurized to the initial pressure P_0, the liquid metal should be near the bottom of the sample tube. After the gas within the sample tube begins to vent into the atmospheric pressure reservoir, the pressure in front of the meniscus will begin to decrease and the liquid metal will rise into the tube. Once the liquid metal reaches the preform, it enters when the pressure difference driving the flow exceeds the minimum capillary pressure for infiltration. As the metal flows through the preform, the infiltration front should move in accordance with fluid flow laws, which predict an increase in infiltration distance proportional to the square root of time at constant applied pressure for both saturated and unsaturated flow.[8-10] Because the liquid metal can enter the preform before the pressure difference driving the flow has reached its full value, it may take some time to develop the proportionality between voltage and time characteristic of the applied pressure difference. At the end of the experiment, the sample space is repressurized, stopping the flow of metal in the preform.

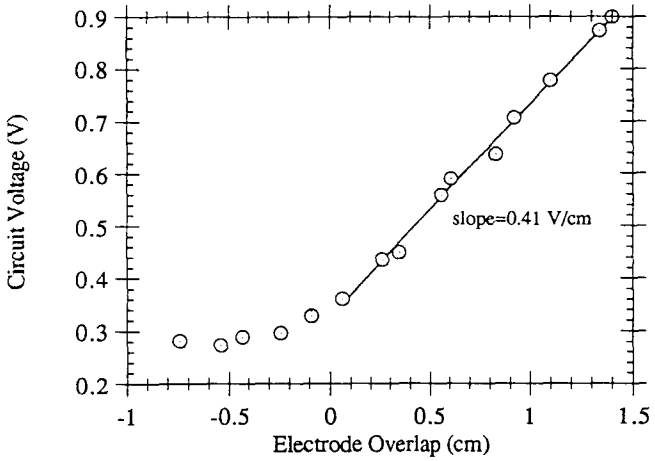

Fig. 4 Typical simulation. This figure illustrates the linear relationship between circuit voltage and electrode overlap for a typical simulation experiment. The line shown was obtained from a least-squares fit.

5.2 *Infiltration of Alumina Preforms*

5.2.1 Infiltration Curve Results

A plateau region of approximately constant circuit signal usually appeared near the beginning of the experiment, typically within a second of the decrease in sample line pressure. In some experiments, the initial signal level was significantly lower than this plateau value, and a rapid transition between the two levels was observed, as shown in Fig. 6. In other experiments, the initial signal level was approximately at or above the plateau value, as illustrated by Fig. 7. In both figures, the pressure difference plotted is the difference between the pressure in the chamber and the sample line at the lid. This pressure difference will be different than that driving the flow if the pressure in the preform is higher than that at the preform exit.

As the two figures illustrate, some time could be required for the plateau value to stabilize. Typically, the plateau was not

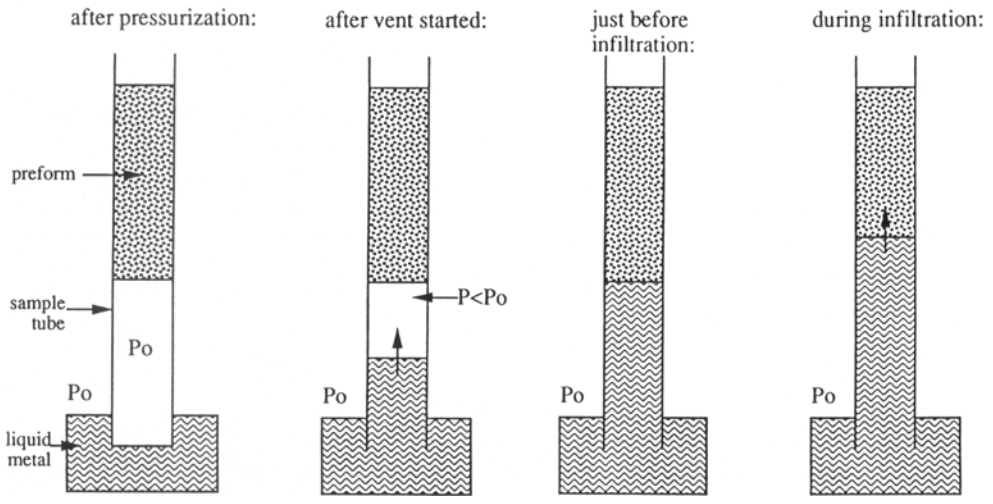

Fig. 5 Physical stages in the infiltration experiment. At the start of the experiment, the liquid metal is at the bottom of the tube. As gas begins to vent from the sample tube, the metal will begin to advance into the tube. However, the metal will not start to enter the preform until the pressure at the preform entrance is less than $P_0 - \Delta P_c$.

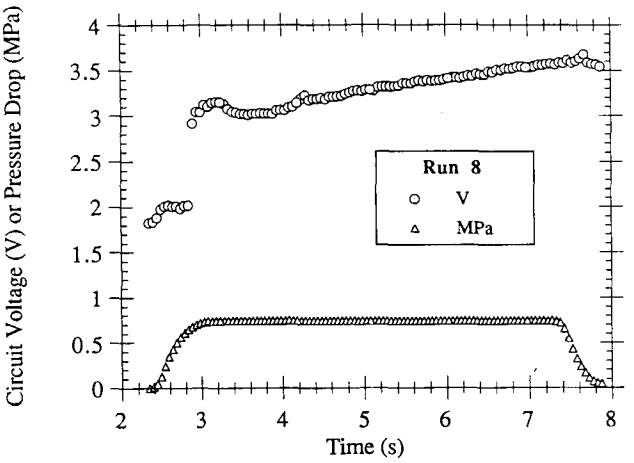

Fig. 6 Low initial signal level. Circuit voltage and pressure difference versus time obtained for an experiment with a low initial signal level. The pressure difference is defined in the text. Run 8: Al-2.3 wt% Mg at 750 ± 5 °C in Ar.

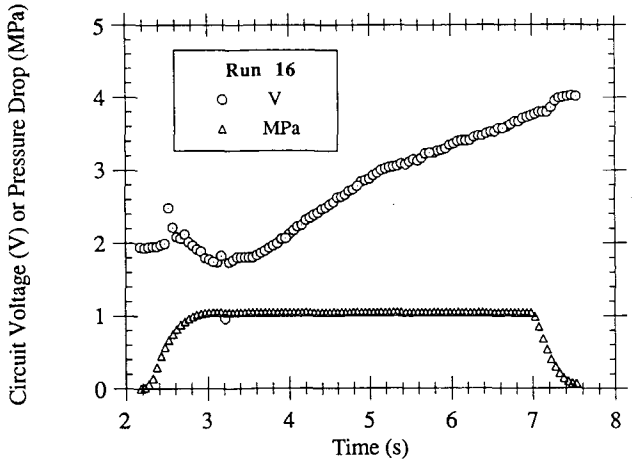

Fig. 7 High initial signal level. Circuit voltage and pressure difference versus time for an experiment with a high initial signal level. The pressure difference is defined in the text. Run 16: Al-5.8 wt% Mg at 750 ± 5 °C in Ar.

completely flat. When the signal was oscillating, the plateau value was taken as the average of the upper and lower oscillation values and the uncertainty as the difference between the average and the extreme values. When the signal trend was either increasing or decreasing, the last value before infiltration appeared to begin was taken as the most likely value, and uncertainty was assigned based on the magnitude of the preceding trend. Relatively well-defined plateau values were found for most experiments. Those experiments without well-defined plateau values were not useful for further analysis.

After some time, the plateau region ended, and the circuit signal began to increase. Often, the increase began several seconds after the start of the experiment. The increase usually occurred after the pressure transducer at the lid of the pressure vessel indicated atmospheric pressure. As Fig. 6 and 7 indicate, the rate of signal increase generally became roughly proportional to the square root of time. The increase was not always smooth; only those experiments showing a relatively smooth increase were analyzed. Sometimes, the gradual rise in signal was interrupted by a rapid jump, as illustrated in Fig. 8. Examination of the preforms from these experiments revealed the formation of an unstable infiltration front, which usually confined itself to the edge of the preform near the tube wall, as shown in Fig. 9. Therefore, only the information before the rapid rise in signal was considered representative of the infiltration process.

After the experiment was stopped and the pressure in the sample space began to increase, the circuit voltage generally began to level off. Occasionally, the signal made a sudden jump up or down. The signal value taken as representative of the end of the experiment was the average of the maximum and minimum values observed after the pressure in the sample space began to increase and before any jump in signal occurred. For those samples with an unstable infiltration front, the representative end value was taken as that present before the rapid rise in signal occurred.

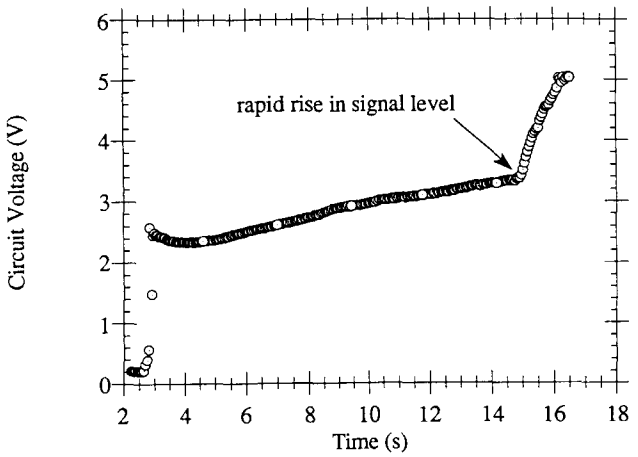

Fig. 8 Rapid signal rise for an unstable front. An example of the rapid rise in signal level associated with the formation of an unstable infiltration front. Run 6: Al at 750 ± 10 °C in Ar.

5.2.2 Discussion of Infiltration Curves

The observed plateau in the signal near the beginning of the experiment was assumed to correspond to the metal front reaching the start of the preform. The plateau probably resulted from the liquid metal being stopped at the entrance of the preform until the pressure within the preform became low enough for the metal to enter. Calculations of the pressure at the preform entrance as a function of time support this explanation.[5] From the discussion presented in Section 5.1, the signal was expected to be low at the beginning of the experiment and then increase to the value corresponding to the start of the preform. However, for some experiments, the initial signal was approximately at the plateau value. The high initial signal level could have been caused by traces of metal left within the tube from the evacuation steps. Such traces were observed for a run that was stopped after evacuation.

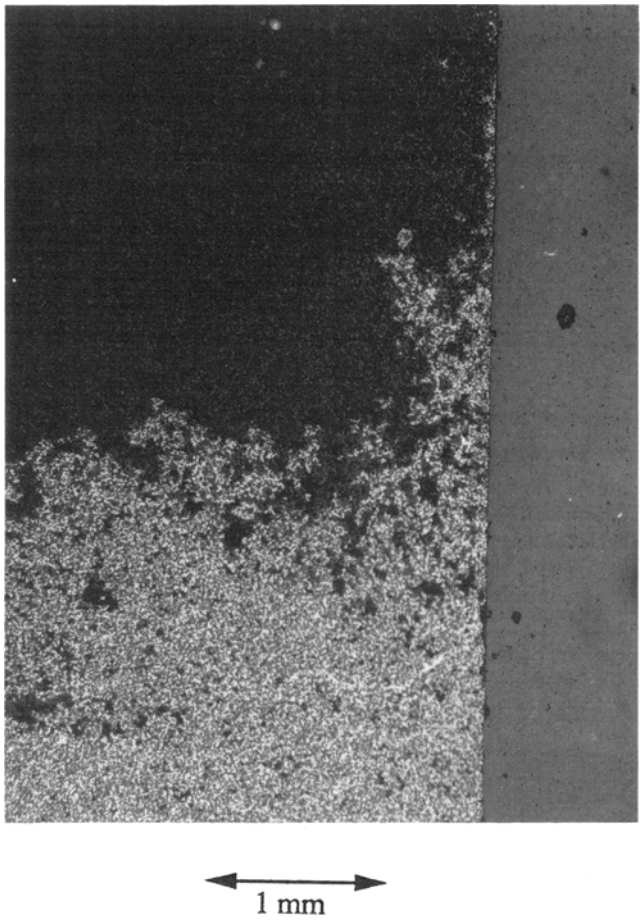

Fig. 9 Formation of an unstable infiltration front along the wall of the sample tube at right. The dark regions at left are areas of the preform that were not infiltrated with metal during the experiment. The light areas indicate infiltrated regions. The main portion of the infiltration front is shown near the bottom of the photograph. Note the projection of the infiltration front near the tube wall, particularly in the upper half of the photograph. Infiltration signal is shown in Fig. 8. Run 6: Al at 750 ± 10 °C in Ar.

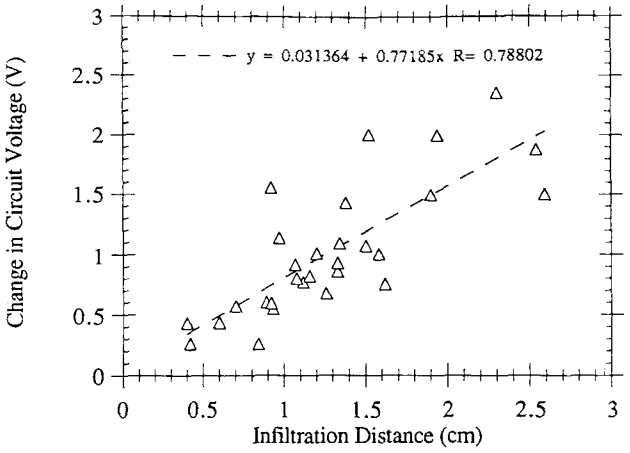

Fig. 10 Circuit voltage versus infiltration distance. Correspondence between changes in circuit voltage and final infiltration distance for different experiments. The line shown was obtained from a least-squares fit through the points.

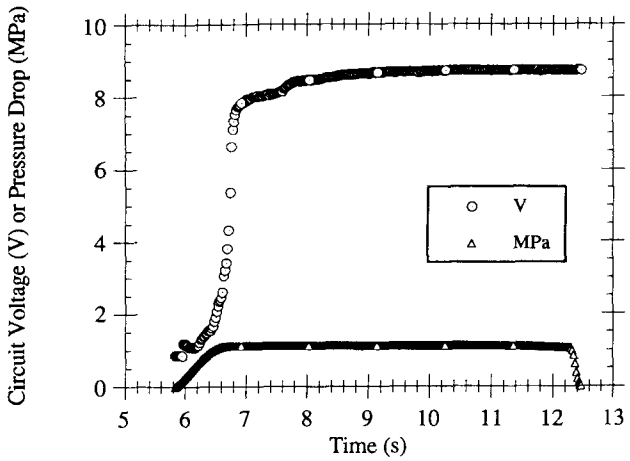

Fig. 11 Silicon carbide infiltration signal. Typical circuit voltage and pressure difference versus time for infiltration of a SiC preform. Run 022391n2: Al-12 wt% Si at 750 °C in air.

Because the stable platcau value was sometimes lower than preceding circuit voltage values, it is likely that not all the changes in signal taking place at the start of the experiment were due to changes in position of the liquid metal inside the sample tube. Transient changes in the signal were also observed at the end of the experiment. The speed or direction of most of the changes made it unlikely that they were due to changes in metal position. One possible explanation is that the flow of metal up the empty portion of the tube at the start of the experiment and the re-equalization of pressure at the end of the experiment may physically move the sample tube with respect to the electrodes, producing a change in capacitance. However, because most of the effects at the beginning of the experiment appear to disappear before infiltration occurs and the effects at the end of the experiment do not obscure the signal analysis, determination of infiltration distance from capacitance measurements is not seriously affected.

The increase in signal following the plateau then corresponded to infiltration of the preform. The increase in signal approximately proportional to the square root of time was in agreement with expected fluid flow behavior.

5.2.3 Proportionality Between Circuit Voltage and Infiltration Distance

Figure 10 compares the final infiltration distance to the voltage obtained by subtracting the plateau voltage from the end voltage for different experiments. The central length of the main portion of the composite was taken as the infiltration distance. Although Fig. 10 shows some scatter, larger voltage changes are clearly correlated with larger infiltration distances. The ratio of the change in voltage to the infiltration distance, V/L, was calculated and ranged from 0.39 to 1.69 V/cm, with an average value of 0.80 ± 0.27 V/cm.

The observed proportionality between changes in circuit voltage and infiltration distance agrees with the expected behavior of the measurement system. Calculation of expected *V/L* values for the infiltration experiments was complicated by the temperature dependence of the electrode dimensions and the dielectric constant of alumina. The diameters of the sample tubes and the signal electrodes at experimental temperatures were estimated using appropriate values for the thermal expansion of polycrystalline alumina and nickel.[11,12] The calculated elongation values were as follows: 1.38% for Ni at 850 °C, 1.20% for Ni at 750 °C, 0.699% for Al_2O_3 at 850 °C, and 0.605% for Al_2O_3 at 750 °C. The dielectric constant of the pressurizing gas was assumed to be essentially temperature independent. Although the temperature dependence of the dielectric constant of the alumina sample tubes was not known, alumina of similar purity and density has a dielectric constant of approximately 11 at 750 to 850 °C and frequencies of 10^4 to 10^5 Hz.[13]

The experimental values ranged between 1.69 and 0.39 V/cm, with an average of 0.80 V/cm. The highest expected value, calculated using Eq 2, was 3.20 V/cm at both 750 and 850 °C. The lowest expected value was 0.60 V/cm at 750 °C and 0.59 V/cm at 850 °C. Although the experimental values tended to cluster around the lower bound, reasonable agreement was obtained between the observed and calculated values, particularly when the approximate nature of the calculations and their sensitivity to the dimensions of the signal electrode were considered. Lower values of the proportionality constant between circuit voltage and infiltration distance could be produced by lower values of the dielectric constant of alumina or slightly different sample tube or signal electrode dimensions.

5.3 *Infiltration of Silicon Carbide Preforms*

For these experiments, a distinct plateau region was not observed near the start of the experiment. Instead, as illustrated in Fig. 11, the initial region of rapid increase in circuit signal was followed by a region of slower, but definite, increase. The second region was followed by a region where the signal began to increase more rapidly, then leveled off. In the third region, the increase was not proportional to the square root of time because the curve tended to flatten at long times. The time at which the third region began tended to be later than for the alumina experiments.

Because the region where infiltration occurred and the start of the preform could not be clearly identified, it was not possible to definitively interpret the circuit signal to determine infiltration distance as a function of time. One possible explanation is that at 750 °C the conductivity of silicon carbide is high enough to interfere with the capacitance measurement, causing the uninfiltrated regions of the preforms to contribute to the capacitance signal. It is known that the conductivity of silicon carbide increases with temperature.[14,15] The contribution of the uninfiltrated preform to the signal may also depend on the extent to which pressure improves the electrical contact between the particles. As the metal moves up the empty portion of the sample tube and reaches the start of the preform, it will make electrical contact with the particles at the start of the preform and apply pressure to the preform. The applied pressure difference will increase as gas vents from the preform, which could produce an increase in signal due to improved electrical contact between the particles. This might explain why no plateau region was observed. In addition, if uninfiltrated regions of the preform contribute to the signal, the entire length of the preform will appear to be infiltrated before it actually is, which might explain why the signal leveled off at the end of the experiment even though infiltration was not complete.

6. Conclusions

The capacitance technique was extended to higher temperatures. Appreciable conductivity of the preform material at the test temperature can limit the use of the technique. The capacitance technique could not be used to interpret infiltration results for semiconducting silicon carbide preforms at 750 °C. However, the technique could be used to determine the infiltration front position during the infiltration of insulating alumina preforms. The observed range of circuit voltage to infiltration distance ratios agreed with the predicted range for the simulation and the alumina preform infiltration experiments. The formation of unstable infiltration fronts could be detected.

Acknowledgments

The authors would like to thank IST/SDIO-ONR for support under contract No. N00014-90-J-1812 and Norton, Co. for donation of the ceramic powders used in this work.

References

1. L.J. Masur, A. Mortensen, J.A. Cornie, and M.C. Flemings, *Metall. Trans. A*, Vol 20, 1989, p 2549-2557
2. A. Mortensen and T. Wong, *Metall. Trans. A*, Vol 21, 1990, p 2257-2263
3. V.J. Michaud and A. Mortensen, *Metall. Trans. A*, Vol 23, 1992, p 2263-2280
4. T.R. Fletcher, J.A. Cornie, and K.C. Russell, *Mater. Sci. Eng.*, Vol A144, 1991, p 159-163
5. T.R. Jonas, "Infiltration and Wetting of Alumina Particulate Preforms with Aluminum-Magnesium Alloys," Ph.D. thesis, Massachusetts Institute of Technology, 1993
6. L.D. Landau and E.M. Lifshitz, *Electrodynamics of Continuous Media*, Addison Wesley, 1960
7. General Electric Catalog
8. A. Mortensen, L.J. Masur, J.A. Cornie, and M.C. Flemings, *Metall. Trans. A*, Vol 20, 1989, p 2535-2547
9. D. Hillel, *Soil and Water: Physical Principles and Processes*, Academic Press, 1971
10. J.R. Philip, *Soil Science*, Vol 85, 1958, p 278-286
11. Y.S. Touloukian, R.K. Kirby, R.E. Taylor, and P.D. Desai, *Thermal Expansion: Metallic Elements and Alloys, Thermophysical Properties of Matter*, Vol 12, IFI/Plenum, 1975
12. Y.S. Touloukian, R.K. Kirby, R.E. Taylor, and T.Y.R. Lee, *Thermal Expansion: Nonmetallic Solids, Thermophysical Properties of Matter*, Vol 13, IFI/Plenum, 1977
13. W.B. Westphal and A. Sils, Air Force Materials Laboratory, Dielectric Constant and Loss Data, 1972
14. G. Busch, *Helv. Phys. Acta*, Vol 19, 1946, p 167-188
15. R.G. Pohl, *Silicon Carbide*, J.R. O'Connor and J. Smiltens, Ed., Pergamon Press, 1960, p 318